RNA Dependent DNA Replication Fidelity of HIV-1 Reverse Transcriptase: Evidence of Discrimination between DNA and RNA Substrates[†]

Stephen G. Kerr[‡] and Karen S. Anderson*

Department of Pharmacology, 333 Cedar Street, Yale University School of Medicine, New Haven, Connecticut 06520-8066

Received June 10, 1997; Revised Manuscript Received September 11, 1997[⊗]

ABSTRACT: The RNA dependent DNA replication fidelity of HIV-1 reverse transcriptase has been investigated using pre-steady-state kinetics under single turnover conditions. In contrast to previous estimates of low replication fidelity of HIV-1 reverse transcriptase, the present study finds the enzyme to be more highly discriminating when an RNA/DNA template−primer is employed as compared with the corresponding DNA/DNA template−primer. The basis of this selectivity is due to extremely slow polymerization kinetics for incorporation of an incorrect deoxynucleotide. The maximum rates for misincorporation (k_{pol}) of dGTP, dCTP, and dTTP opposite a template uridine were 0.2, 0.03, and 0.003 s^{-1}, respectively. The equilibrium dissociation constants (K_d) for the incorrect nucleotide opposite a template uridine were 1.0, 1.1, and 0.7 mM for dGTP, dCTP, and dTTP, respectively. These kinetic values provide fidelity estimates of 26 000 for discrimination against dGTP, 176 000 for dCTP, and 1×10^6 for dTTP misincorporation at this position. Similar observations were obtained when incorrect nucleotide misincorporation was examined opposite a template adenine. Thus in a direct comparison of RNA/DNA and DNA/DNA template−primer substrates, HIV-1 RT exhibits approximately a 10−60-fold increase in fidelity. This study augments our current understanding of the similarities and differences of catalytic activity of HIV-1 reverse transcriptase using RNA and DNA substrates. Moreover, these studies lend further support for a model for nucleotide incorporation by HIV-1 reverse transcriptase involving a two-step binding mechanism governed by a rate-limiting conformational change for correct incorporation.

HIV-1 reverse transcriptase (RT[1]) is a virally encoded enzyme essential for viral replication and the target of clinically useful drugs for treatment of aquired immunodeficiency syndrome (AIDS). An in-depth understanding of the catalytic mechanism of HIV-1 RT may ultimately aid in the development of better therapeutics.

Pre-steady-state kinetic techniques have been previously employed to determine the mechanism for polymerases and to provide estimates of replication fidelity (Kuchta et al., 1987; Kuchta et al., 1988). Such transient kinetic model systems have also been used to provide mechanistic information for HIV-1 RT (Kati et al., 1992; Reardon, 1992; Reardon, 1993; Hsieh et al., 1993). Earlier mechanistic studies on HIV-1 reverse transcriptase (RT) using rapid transient kinetic analysis suggest that catalysis at the active site is similar to other polymerases such as T7 DNA polymerase (Patel et al., 1991; Wong et al., 1991) involves an "induced fit" model for polymerization (Kati et al., 1992, Hsieh et al., 1993). Although the proposal of a two-step binding model involving a rate-limiting conformational change (Kati et al., 1992) has been challenged (Reardon, 1993), more recent transient kinetic studies on HIV-1 RT substantiate the validity of this model (Spence et al., 1995; Rittinger et al., 1995). This model describes the reaction pathway for deoxynucleotide triphosphate (dNTP) incorporation for HIV-1 RT in terms of a two-step binding process (Kati et al., 1992; Hsieh et al., 1993; Spence et al., 1995; Rittinger et al., 1995). The first step in dNTP binding comprises an initial binding complex in which the dNTP is base paired with the requisite base in the template strand. In the second step the enzyme checks for proper base pairing geometry in which only correct base pairs may induce the formation of a tight ternary complex leading to catalysis. The maximal rate of polymerization is governed by a rate-limiting conformational change which precedes the chemical catalytic step and is observed with both DNA/DNA template−primer substrates as well as RNA/DNA template−primer substrates.

This two-step mechanism controls the selectivity for correct versus incorrect dNTP incorporation. Whereas T7 DNA polymerase is considered to exhibit high DNA replication fidelity (Johnson, 1993), HIV-1 RT has been reported to have a low DNA replication fidelity (Preston et al., 1988; Roberts et al., 1988; Weber et al., 1989; Bebenek et al., 1989; Ji and Loeb, 1992, 1994; Perrino et al., 1989; Mendelman et al., 1989; Mendelman et al., 1990; Yu et al., 1992; Preston et al., 1997). The low estimates for DNA fidelity are based upon analysis of mutation frequency using assays involving transfection (Preston et al., 1988; Roberts et al., 1988; Weber et al., 1989; Bebenek et al., 1989; Ji and Loeb, 1992; Perrino et al., 1989) or steady-state kinetic gel shift systems (Preston et al., 1988; Mendelman et al., 1989; Mendelman et al., 1990; Ricchetti and Buc, 1990; Yu et al., 1992). Error-prone

[†] This work was supported by NIH Grant GM 49551 to K.S.A.

* Author to whom correspondence should be addressed. Telephone: (203)-785-4526. Fax: (203)-785-7670. email: karen.anderson@yale.edu.

[‡] Present address: Massachusetts College of Pharmacy & Allied Health Sciences, 179 Longwood Ave., Boston, MA 02115.

[⊗] Abstract published in *Advance ACS Abstracts,* November 1, 1997.

[1] Abbreviations used: dNTP, deoxynucleoside 5′-triphosphate; dATP, deoxyadenosine 5′-triphosphate; dCTP, deoxycytidine 5′-triphosphate; dGTP, deoxyguanosine 5′-triphosphate; dTTP, deoxythymidine 5′-triphosphate; EDTA, ethylenediaminetetraacetic acid; HIV-1, human immunodeficiency virus type 1; RT, reverse transcriptase.

S0006-2960(97)01385-8 CCC: $14.00

polymerization of RT has also been described in terms of errors initiated by template−primer misalignments (Roberts et al., 1988; Bebenek et al., 1989; Bebenek et al., 1993). These studies have provided insight toward our understanding of the biologically important reactions contributing to observed mutation frequencies. However, these studies do not provide a detailed mechanistic picture concerning how HIV-1 RT accommodates both RNA/DNA and DNA/DNA duplexes and controls DNA replication fidelity.

A rapid transient kinetic approach will provide an in-depth mechanistic understanding of factors governing replication fidelity for DNA dependent and RNA dependent polymerization. The DNA dependent replication fidelity of HIV-1 RT has been examined using rapid transient kinetic analysis (Kati et al., 1992; Zinnen et al., 1994). In an effort to further understand the similarities and differences for the catalytic activity of HIV-1 RT in utilizing DNA and RNA substrates, the present study was undertaken to examine the RNA dependent DNA replication fidelity of HIV-1 RT. The biological implications are important since it is likely that the RNA dependent DNA replication fidelity may play an essential role in successful viral survival.

In this report we provide a comparison of replication fidelity using DNA/DNA and RNA/DNA template−primer substrates. The fidelity estimates provided in this study reveal differences in DNA and RNA substrates and lend further support for an induced fit mechanism in which conformational coupling plays an important role in polymerase fidelity (Johnson, 1993).

EXPERIMENTAL PROCEDURES

Overexpression and Purification of Recombinant HIV-1 RT. In these experiments, RT was purified from a clone generously provided by Barbara Müller and Roger Goody which expresses both subunits (66 and 51 kDa) of the protein (Müller et al., 1989). The *Escherichia coli* cells were grown up in 2× YT broth containing ampicillin (100 mg/L) at 37 °C for 4 h to an optical density of 0.5 unit at 595 nm. The growth was then induced by the addition of IPTG (1 mM), and the cells were allowed to grow for an additional 5−6 h. All purification steps were done in the cold, 0−4 °C. Cells were harvested by centrifugation at 4 °C and resuspended in buffer A (50 mM Tris-Cl, pH 8.0, 2 mM EDTA, 2 mM dithiothreitol, 1 mM phenylmethanesulfonyl fluoride, 10% glycerol) containing 0.5 M NaCl and 0.1% Triton X-100. The cells were lysed using a french pressure cell press (SLM Instruments) at 20 000 psi. The lysed cells were centrifuged at 15 000 rpm. The supernatant was decanted and the pellet extracted once more with the lysis buffer followed by centrifugation. The two supernatants were combined and nucleic acids precipitated by addition of 5% poly(ethyleneimine) to a final concentration of 0.3%. The precipitated nucleic acids were removed by centrifugation at 10 000 rpm. To the supernatant was then added ammonium sulfate (60%). Crude precipitated protein was centrifuged, resuspended, and dialyzed against buffer A. Crude RT was purified by column chromatography over a phosphocellulose column (Waters) using a linear gradient of 0.05−1 M NaCl in buffer A. Fractions containing RT were pooled and dialyzed against buffer A and subsequently loaded onto a Q-Sepharose (Pharmacia) column. RT was eluted using a linear gradient from 10 to 250 mM NaCl. The pooled RT fractions were combined, concentrated, and further purified by strong cation exchange FPLC using a Mono S 5/5 column (Pharmacia) as previously described (Stahlhut et al., 1994). This step has been shown to separate homodimeric p66 and p51 species from p66/p51 heterodimer and provide the desired heterodimer in a 1:1 ratio. The RT was dialyzed against buffer A containing 50 mM NaCl, concentrated, aliquoted, and stored at −70 °C. Enzyme concentration was estimated by UV at 280 nm using an extinction coefficient of 260 450 M^{-1} cm $^{-1}$ as previously described (Kati et al., 1992). Concentrations of RT used in subsequent experiments were determined by an active site titration method as previously described (Kati et al., 1992). The preparation of RT with this system and purification procedure gave burst amplitudes of 30−40%, and the enzyme concentrations for all experiments were performed using the corrected active concentration. The RT obtained after this purification procedure was highly pure and free of contaminating exonuclease or RNAse activities. The exonuclease activity was judged by incubation of enzyme with radiolabeled DNA/DNA 45−25-mer for 30 min at 37 °C and the RNase activity was evaluated by incubation of enzyme with radiolabeled RNA 45-mer for 30 min at 37 °C. In each case <5% of the substrate was degraded to cleavage products.

Table 1: RNA and DNA Oligonucleotides Substrates

45/25 template primer:

RNA

CGGAGCGUCGGCAGGUUGGUUGAGUUGGAGCUAGGUUACGGCAGG-5'

GCCTCGCAGCCGTCCAACCAACTCA-3'

DNA

CGGAGCGTCGGCAGGTTGGTTGAGTTGGAGCTAGGTTACGGCAGG-5'

GCCTCGCAGCCGTCCAACCAACTCA-3'

45/22 template primer:

RNA

CGGAGCGUCGGCAGGUUGGUUGAGUUGGAGCUAGGUUACGGCAGG-5'

GCCTCGCAGCCGTCCAACCAAC-3'

DNA

CGGAGCGTCGGCAGGTTGGTTGAGTTGGAGCTAGGTTACGGCAGG-5'

GCCTCGCAGCCGTCCAACCAAC-3'

Nucleotide Triphosphates and Other Materials. All dNTPs were obtained from Pharmacia LKB Biotechnology Inc. and determined to be >99% pure by anion-exchange HPLC. [γ-^{32}P]ATP was obtained from Amersham Co. Biospin columns for purification of labeled oligomers were obtained from BioRad.

Synthetic Oligonucleotides. The DNA 25-mer and 22-mers (Table 1) were synthesized on an Applied Biosystems 380A DNA synthesizer from the Yale DNA Synthesis Facility and purified by denaturing polyacrylamide gel electrophoresis (16%) as previously described (Kati et al., 1992). RNA 45-mer (Table 1) was obtained from the Yale Synthesis Facility and purified as described (Kati et al., 1992) or obtained as the deprotected gel and HPLC purified material from New England Biolabs, Inc.

The heteroduplex RNA/DNA 45/25-mer template−primer strands were annealed using equimolar ratios of pure template−primer at 80 °C for 4 min and 50 °C for 30 min

as previously described (Kati et al., 1992). Concentrations of the oligomers were estimated from UV absorbances at 260 nm using extinction coefficients of 507 960 and 249 040 M^{-1} cm^{-1} for the RNA 45-mer, and DNA 25-mer, respectively. The corresponding extinction coefficient for the DNA 22-mer was 218 390 M^{-1} cm^{-1}.

Buffers. All experimental procedures involving kinetic experiments of RT were done in 50 mM Tris-Cl, 50 mM NaCl, pH 7.5 at 37 °C, and used sterile buffers, reagents, and laboratory ware wherever possible.

5′-[^{32}P]-Labeling the 45/25-mers and 45/22-mers. The RNA 45-mer, DNA 25-mer, and DNA 22-mer strands were 5′-labeled with [γ-^{32}P]ATP using T4 polynucleotide kinase (New England Biolabs, Inc.) according to previously described procedures (Kati et al., 1992).

Rapid Quench Experiments. Rapid quench experiments were carried out in an apparatus designed by Johnson (Johnson, 1986; Johnson, 1992) and built by Kintek Instruments (State College, PA). The apparatus was modified to allow small reaction volumes of 15 μL. Experiments were carried out as described (Kati et al., 1992). Briefly, 15 μL of substrate (RNA or DNA template−primer) preincubated with enzyme (RT) was loaded in one sample loop while the other loop contained an equal amount of the nucleotide to be incorporated, preincubated with Mg^{2+}. Enzyme catalysis was initiated by rapidly mixing the two reactants together and was terminated by quenching with 0.3 M EDTA (final concentration) after time points ranging from milliseconds to several seconds. In the cases where long reaction times were required (as in the case for dTMP incorporation), manual quench experiments were undertaken in which the two solutions (substrate preincubated with RT and dTTP-Mg^{2+}) were incubated at 37 °C, and at regular time intervals 30 μL of the reaction solution was removed and quenched with EDTA (0.3 M final concentration). All concentrations reported in the text are final concentrations after mixing.

Product Analysis. The products were analyzed by sequencing gel analyses (16% polyacrylamide gel in 8 M urea) where elongation products from the primer strand and the template strand and its degradation products could be resolved and quantitated. The products and substrates were quantitated by scanning the dried gel using a either a GS-250 Molecular Imager System (BioRad) or Betascope (Betagen).

Data Analysis. Data were fit by nonlinear regression analysis using the commercially available program KaleidaGraph (Synergy Software, Reading, PA) for the Macintosh computer. The data were fit to a burst equation, product = $A(1 - \exp(-kt)) + mt$, where A is the amplitude of the burst, k is the observed first-order burst rate constant, and m is the linear steady-state rate constant; for pre-steady-state bursts experiments or, to a single exponential, product = $A(1 - \exp(-kt))$ according to the mechanism previously described (Kati et al., 1992). The concentration dependence of the burst rate were fit to a hyperbolic function in which $k = k_{pol}[dNTP]/(K_d + [dNTP])$, where k is the observed rate, k_{pol} is the maximum rate of incorporation and K_d is the equilibrium dissociation constant for the dNTP. The term k_{pol} is used even in cases where the rates are extremely slow since under single turnover conditions the observed rate is still a function of the maximum rate of nucleotide incorporation. Since k_{pol} is most likely defined by a slow conformational or chemical step, and not product release, it would be equivalent to k_{cat}.

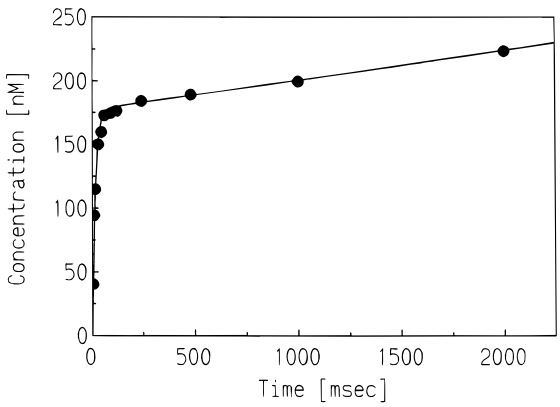

FIGURE 1: Pre-steady-state kinetics of correct incorporation of dATP, U·dA base pair. Pre-steady-state kinetics of correct incorporation of dATP into heteroduplex RNA/DNA 45/25-mer (template−primer) were measured by mixing a preincubated solution of RT (175 nM active site concentration) and 5′-[^{32}P]-labeled RNA/DNA (300 nM) with Mg^{2+} (10 mM) and dATP (200 μM) under rapid quench conditions. The reactions were quenched with 0.3 M EDTA at the indicated times, and the product 26-mer primer was separated and quantitated by sequencing gel analysis (16% acrylamide, 8 M urea). The solid line represents the best fit of the data (●) to a burst equation with rate constants equal to 68 and 0.13 s^{-1} for the exponential and linear phases, respectively.

RESULTS

In this report we contrast the RNA dependent and DNA dependent replication fidelity of recombinant HIV-1 reverse transcriptase by examining the kinetics of incorrect nucleotide incorporation into a RNA/DNA template−primer as compared with the corresponding DNA/DNA template−primer substrate. Studies were conducted with two synthetic oligonucleotide substrates: a 45/25 template−primer and a 45/22 template−primer (shown in Table 1) . For the 45/25 template−primer, the mismatch involved incorporation of an incorrect dNTP (dGTP, dCTP, and dTTP) opposite a template uridine (U). This analysis was extended to a 45/22 template−primer to examine the incorporation of an incorrect dNTP (dGTP, dCTP, and dATP) opposite a template adenosine (A). The polymerization rate constants (k_{pol}) and equilibrium dissociation constants (K_d) of the incorrect dNTPs have been determined. From these kinetic parameters, fidelity estimates for the RNA dependent DNA polymerization have been calculated. The results are compared and contrasted with the fidelity estimates of DNA dependent DNA polymerization (Kati et al., 1992).

Pre-Steady-State Kinetic Studies Using a 45/25 Template−Primer

Correct Incorporation of dATP into Heteroduplex RNA/DNA 45/25 Template−Primer. We began our studies examining RNA dependent replication fidelity by determining the kinetic parameters for correct dNTP incorporation to provide a framework for comparison of incorrect incorporation. A representative pre-steady-state burst experiment for the correct incorporation of dATP is shown in Figure 1. The experiment was performed by mixing a preincubated solution of RT (175 nM active site concentration) and 5′-[^{32}P]-labeled RNA/DNA 45/25-mer (300 nM) with Mg^{2+} (10 mM) and dATP (200 μM), the nucleotide for correct

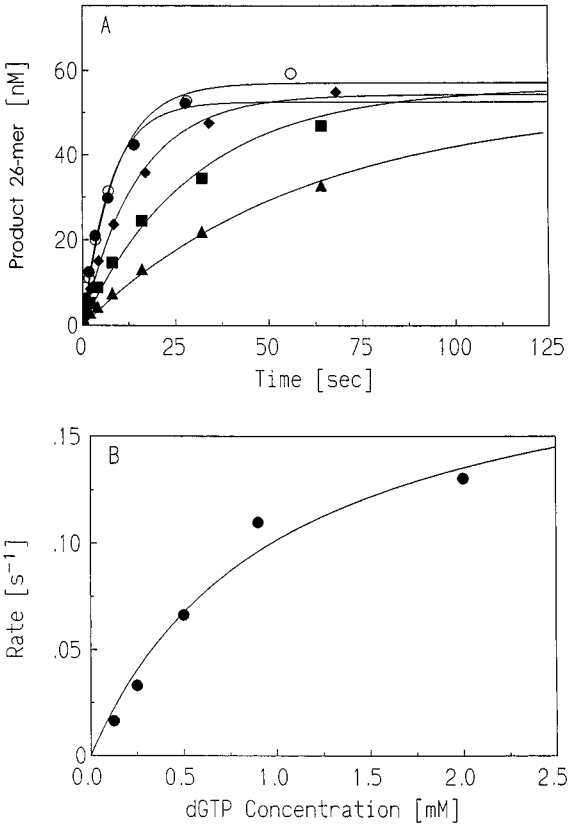

FIGURE 2: dGTP concentration dependence on the first-order rates for misincorporation, U·dG mismatch. (A) A preincubated solution of RT (100 nM) and 5′-[^{32}P]-labeled 45/25-mer RNA/DNA (90 nM) was mixed with increasing concentrations of dGTP in Mg^{2+} buffer to start the reactions. The reactions were quenched with 0.3 M EDTA at the indicated times, and the products were analyzed and quantitated as indicated previously. The dGTP concentrations were (▲) 0.125 mM; (■) 0.25 mM; (♦) 0.5 mM; (○) 0.9 mM; (●) 2 mM. The solid lines represent the best fit of the data to the first-order processes. (B) The first-order rates (●) measured above were plotted against the dGTP concentrations. The fit to a hyperbola yielded a K_d value of 1 ± 0.3 mM for dGTP dissociation and a maximum rate of misincorporation of 0.203 ± 0.03 s^{-1}.

incorporation. The resulting time course of dATP incorporation (Figure 1) showed biphasic kinetics with the first turnover occurring at a rate (k_{pol}) of 68 s^{-1} and subsequent turnovers at a rate (steady-state rate) of 0.13 s^{-1} similar to our previous results (Kati et al., 1992). Likewise, biphasic kinetics were also observed for the correct incorporation of dTTP into an RNA/DNA or DNA/DNA 45/22 template−primer (see below).

Misincorporation of dNTP into RNA/DNA 45/25-mer. The kinetics of misincorporation of the three deoxynucleoside triphosphates, dGTP, dCTP, and dTTP, into the heteroduplex RNA/DNA 45/25-mer were determined. The experiments with dGTP and dCTP required the use of a rapid quench apparatus while those for dTTP were conducted by manual quench. The equilibrium dissociation constants, K_ds, and maximum rates of incorporation, k_{pol}, of the three incorrect dNTPs were determined under single turnover conditions with enzyme (RT 100 nM) in slight excess of substrate (RNA/DNA, 90 nM) and quantitating all products formed. Substrate inhibition occurred with dNTP concentrations in excess of 2 mM as previously observed (Kati et al., 1992).

(a) Misincorporation of dGTP: Kinetics of a U·dG Mismatch. Figure 2A shows the concentration dependence on the first-order rates of incorporation of dGTP into the primer 25-mer strand opposite a template uridine. Reactions were carried out as indicated in the figure legend. The misincorporation of dGTP led to the elongation of the 25-mer by one base to form a 26-mer product. The formation of the 26-mer product was quantified and plotted versus time. The data for each time course was fit to a single exponential to provide the rate of polymerization. Figure 2B is a plot of the first-order rates, determined above, versus dGTP concentration (mM) and fit to a hyperbola to determine, k_{pol}, the maximum rate of incorporation (0.203 ± 0.03 s^{-1}), and the dissociation constant, K_d, for dGTP (1 ± 0.3 mM) for the U·dG mismatch.

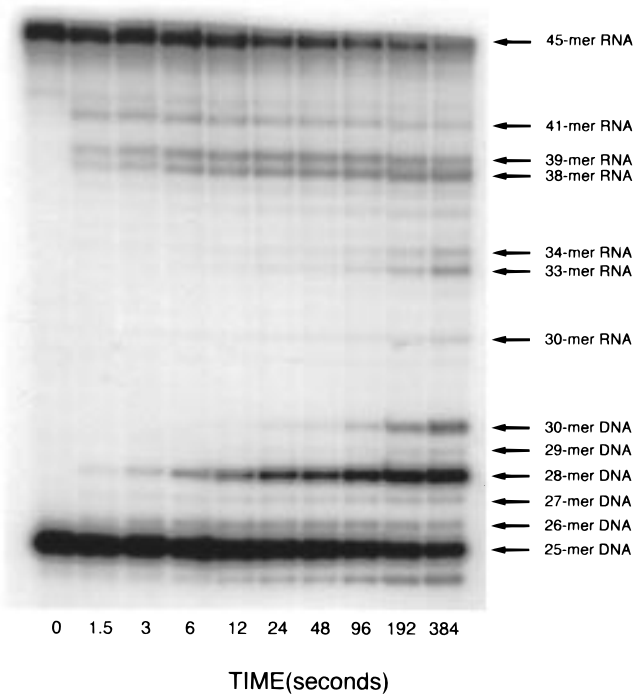

FIGURE 3: Gel analysis of misincorporation of dCTP into RNA/DNA 45/25-mer, a U·dC mismatch. The bands indicate the time course (0−384 s) of polymerization of the 45/25-mer RNA/DNA heteroduplex (90 nM) by RT (100 nM) in presence of dCTP (1.25 mM) and Mg^{2+} (10 mM). Polymerization product bands are at 26-, 27-, 28-, 29-, and 30-mer (see text for explanation). The product was quantitated by the summation of all product bands (26−30-mer) for the individual time courses. The RNA template 45-mer is also visible along with the RNA cleavage fragments at 39- and 38-mer and smaller, depicting the simultaneous RNAse H activity of HIV-1 RT. These cleavage fragments are similar to those seen previously (Kati et al., 1992) and confirm the distance between the polymerase and RNAse H sites to be approximately 18−19 nucleotides apart.

(b) Misincorporation of dCTP: Kinetics of a U·dC Mismatch. Similar experiments to those done above for dGTP were conducted to obtain the dissociation constant and an estimate of the maximum rate of incorporation of dCTP opposite a template uridine. The incorporation of dCTP led to a series of five bands of sizes 26−30 bases. This resulted from the fact that after the initial misincorporation of dCMP to form DNA 26-mer, dCTP is the correct nucleotide for the next two additions (27- and 28-mers). At higher concentrations and longer time points, a second misincorporation on the 28-mer generates a 29-mer, and since dCTP is again the correct nucleotide for the next addition, a 30-mer accumulates. The gel analysis of the time course of the reaction of a preincubated solution of RT (100 nM) and 5′-[32P]-doubly-labeled 45/25-mer RNA/DNA (90 nM) with

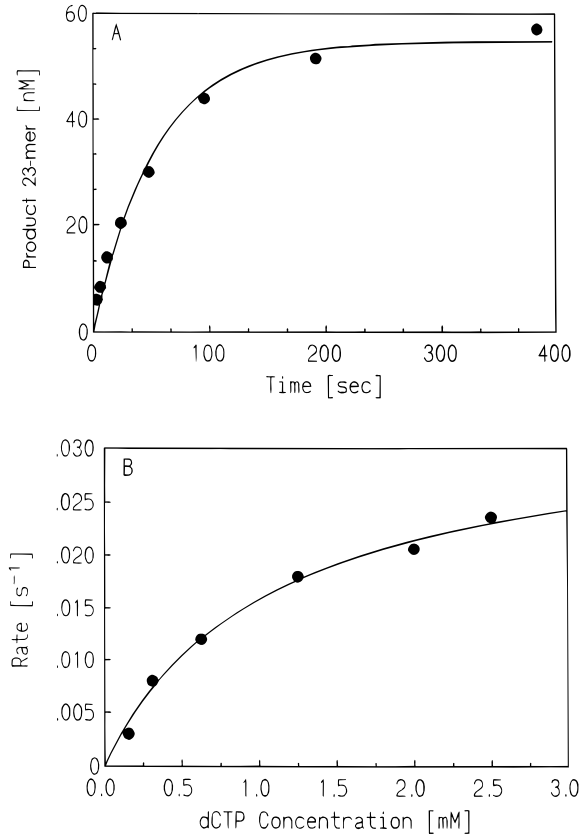

FIGURE 4: Misincorporation of dCTP into RNA/DNA 45/25-mer, U·dC mismatch. (A) A preincubated solution of RT (100 nM) and 5′-[^{32}P]-labeled 45/25-mer RNA/DNA (90 nM) was mixed with dCTP (1.25 mM) in Mg^{2+} buffer to start the reaction. The reaction was quenched with 0.3 M EDTA at the indicated times, and the products were analyzed and quantitated as indicated in the text. The solid line represents the best fit of the data (●) under single turnover conditions, using a rate constant of 0.018 s^{-1} for the first-order exponential process. (B) The first-order rate constants determined analogously to the above experiment, with varying concentrations of dCTP, were plotted against the dCTP concentrations. The data (●) were fit to a hyperbola (solid line) to yield a K_d value of 1.11 ± 0.15 mM for dCTP dissociation and a rate of misincorporation of 0.033 ± 0.002 s^{-1}.

dCTP (1.25 mM) in Mg^{2+} buffer is shown in Figure 3. The major polymerization products (dark bands) of 28-mer and 30-mer, where the reaction has stalled, are clearly visible, while faint bands of the 26-mer, 27-mer, and 29-mer can also been seen. Other bands seen are those from the RNAse H cleavage reaction (see Discussion below). All five bands were summed and quantified to yield total products, thus defining the kinetics of the first misincorporation (Wong et al., 1991; Kati et al., 1992). Thus, from a plot of total products (26−30-mer) formed versus time and fitting the plot to a first-order (single turnover) equation, one can obtain a lower limit for the rate of dCTP incorporation, Figure 4A. From a plot of the rate constants of dCTP incorporation versus dCTP concentration and fitting the data to a hyperbola, the lower limit for maximum rate of incorporation of the U·dC mismatch was determined to be 0.033 ± 0.002 s^{-1} and K_d for dCTP was 1.1 ± 0.15 mM, Figure 4B.

(c) Misincorporation of dTTP: U·dT Mismatch. Identical experiments to those conducted for dCTP and dGTP were conducted for determining the incorporation rate for a U·dT mismatch. The maximum rate of incorporation was determined to be 0.0034 ± 0.0004 s^{-1} and K_d for dTTP dissociation was 0.7 ± 0.18 mM for the U·dT mismatch.

Table 2: Fidelity of HIV-1 RT with 45/25 Template−Primer

dNTP	K_d (μM)	k_{pol} (s^{-1})	k_{pol}/K_d (μM^{-1} s^{-1})	fidelity[a] (RNA)	fidelity[b] (RNA)
dATP	14	74 (33)	5.28		
dGTP	1000	0.2 (4.8)	2.0×10^{-4}	26 000	1740
dCTP	1100	0.03 (0.05)	3.0×10^{-5}	176 000	19 700
dTTP	700	0.003 (0.4)	4.9×10^{-6}	1 100 000	16 900

[a] Calculated as $[(k_{pol}/K_d)_{correct} + (k_{pol}/K_d)_{incorrect}]/(k_{pol}/K_d)_{incorrect}$. [b] Kati et al., 1992; values in parentheses for k_{pol} are the rates of incorporation for the DNA template.

Striking differences are noted between the rates of misincorporation for the RNA template as compared with DNA for each of the mismatches examined as shown in Figure 5. This figure visually illustrates these findings by showing a gel analysis directly comparing misincorporation of dTMP using the RNA 45-mer template (right) with the DNA 45-mer template (left). At the 40 s time point, most of the 25-mer has been converted to 26-mer for the DNA while only a trace of 26-mer is seen with the RNA template. Also shown in Figure 5 are the anticipated RNAase H cleavage products (RNA 38-mer and 39-mer) as discussed below.

Fidelity Estimates. Table 2 summarizes the kinetic parameters for correct and incorrect incorporation into the heteroduplex RNA/DNA 45/25 template−primer. The RNA dependent DNA replication fidelity was estimated from the ratios of incorporation of the second-order rate constants of correct to incorrect, as calculated by the expression shown in Table 2. Fidelity estimates for the U·dG, U·dC, and U·dT mismatches were 26 000, 176 000, and 1 000 000, respectively. The corresponding estimates for k_{pol} (shown in parentheses) and DNA dependent replication fidelity for the DNA/DNA 45/25 template−primer are also shown for comparison.

Pre-Steady-State Kinetic Studies Using a 45/22 Template−Primer

Although the higher fidelity for an RNA/DNA template−primer compared to a DNA/DNA template−primer in the case of a 45/25 template−primer was interesting, the generality of this observation was uncertain. Therefore, analysis of a 45/22 template−primer was undertaken to examine the correct and incorrect incorporation of dNTP opposite a template adenosine (A) using the DNA and RNA substrates shown in Table 1. The equilibrium dissociation constants, K_ds, and maximum rates of incorporation, k_{pol}, for the correct and three incorrect dNTPs were determined under single turnover conditions analogous to that described above for the 45/25 template−primer. The kinetic parameters, K_d and k_{pol}, and fidelity estimates for the A·dC, A·dA, and A·dG mismatches using a DNA or RNA substrate are shown in Table 3. The estimates for DNA dependent replication fidelity for a dC, dA, and dC mismatch were 800, 150 000, and 350 000. For the corresponding RNA dependent replication fidelity for dC, dA, and dC mismatches, the estimates were 12 000, 3 500 000, and 4 600 000. These results suggest that HIV-1 RT is, in general, more highly discriminating toward an RNA/DNA template−primer.

RNase H Activity of RT for Correct versus Incorrect Nucleotide Incorporation. We have previously investigated the simultaneous catalytic activities of DNA polymerization and RNA cleavage by using the 5′-doubly-labeled RNA/

Table 3: Fidelity of HIV-1 RT for 45/22 Template−Primer

	k_{pol} (s^{-1})		K_d (μM)		k_{pol}/K_d (μM^{-1} s^{-1})		fidelity[a]	
dNTP	RNA	DNA	RNA	DNA	RNA	DNA	RNA	DNA
dTTP	72	0.96	17	7	4.2	0.14		
dCTP	0.5	0.29	1400	1700	3.5×10^{-4}	1.7×10^{-4}	12 000	800
dATP	1.3×10^{-3}	9.2×10^{-4}	1100	970	1.2×10^{-6}	9.5×10^{-7}	3 500 000	148 000
dGTP	3.3×10^{-3}	2.7×10^{-3}	3700	6800	9.0×10^{-7}	3.9×10^{-7}	4 700 000	360 000

[a] Calculated as $[(k_{pol}/K_d)_{correct} + (k_{pol}/K_d)_{incorrect}]/(k_{pol}/K_d)_{incorrect}$.

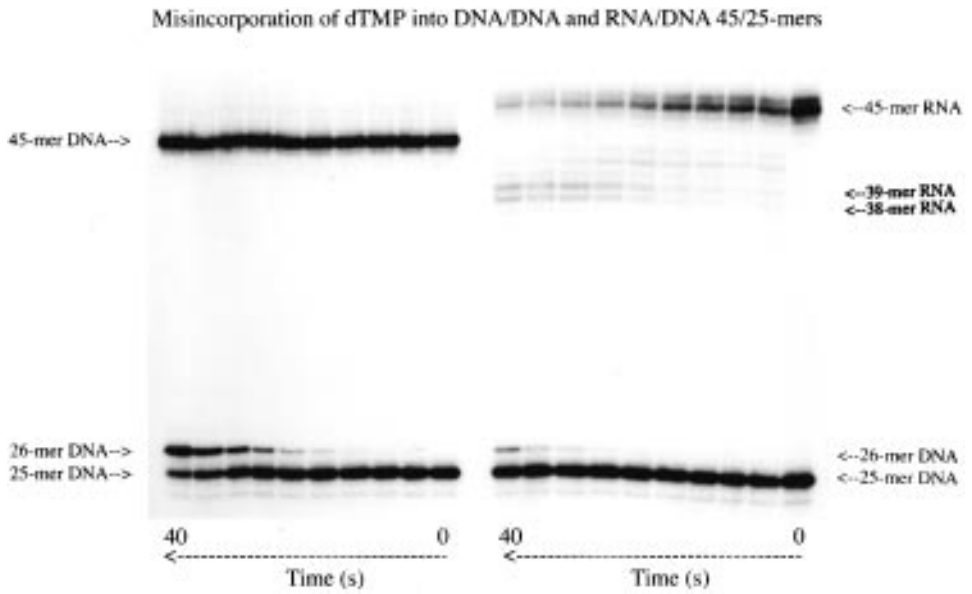

FIGURE 5: Comparison of misincorporation of dTTP into DNA/DNA 45/25-mer (T· dT mismatch) or RNA/DNA 45/25-mer (U·dT mismatch). A preincubated solution of RT (100 nM) and doubly-labeled 5′-[^{32}P]-labeled 45/25-mer DNA/DNA (left) or RNA/DNA (right) (90 nM) was mixed with dTTP (2 mM) in Mg^{2+} buffer to initate the reaction. The time course for the formation of the 26-mer misincorporation product is shown over a period of 40 s. In the case of the DNA substrate , >70% of the product is formed after 40 s; however with the RNA substrate less than 15% of the product is observed at the same reaction time. Thus the catalytic activity of HIV RT for incorporating mismatches is substantially different for RNA versus DNA.

DNA 45/25 template−primer shown in Table 1 (Kati et al., 1992). In the present study we have examined the RNase H activity and sites of template cleavage under conditions of incorrect nucleotide incorporation. The rate of RNase H cleavage ranged from 3 to 16 s^{-1} and appeared to be independent of the rate of polymerization. The site of RNase H cleavage on the template was also independent of the nucleotide (correct or incorrect) being incorporated. This analysis also provided further confirmation of the distance between the polymerase and RNase H active sites (Kati et al., 1992; Gopalakrishnan et al., 1992) by determining the length of RNA cleavage products produced (see Figure 3 and 5). On the basis of the 38- or 39-mer RNA cleavage products obtained, a distance of 19 RNA/DNA heteroduplex bases is suggested between the two sites and is consistent with the three-dimensional structural studies on RT (Kohlstaedt et al., 1992; Jacobo-Molina et al., 1993). As previously shown with correct incorporation, 41-mer RNA cleavage product was also observed which may result from an alternate binding mode. In general, the RNase H catalytic activity was similar to that previously determined for correct nucleotide incorporation (Kati et al., 1992).

DISCUSSION

Previous studies have determined the kinetic parameters of HIV-1 RT for both RNA dependent as well as DNA dependent polymerization (Kati et al., 1992). It was shown that for correct nucleotide incorporation (dATP) into a predefined template−primer 45/25-mer, the RNA dependent polymerization rates (k_{pol}) were at least 2-fold faster than the DNA dependent polymerization rates (74 s^{-1} compared to 33 s^{-1}), while the dissociation constants (K_d) for the incoming nucleotide were essentially similar to that of the deoxynucleotide triphosphate, dATP, showing slightly greater affinity for the DNA/DNA 45/25-mer template−primer (4 μM) compared with the RNA/DNA 45/25-mer (14 μM) (Kati et al., 1992). Fidelity estimates from single turnover experiments for the DNA dependent polymerization were in the range of 1/1700 for misincorporation of dGMP opposite a template thymidine to approximately 1/18000 for misincorporation of either a dCMP or dTMP opposite a template thymidine. The results were in general agreement with other fidelity studies on HIV-1 RT (Preston et al., 1988; Roberts et al., 1988; Weber et al., 1989; Bebenek et al., 1989; Ji and Loeb, 1992; Perrino et al., 1989; Mendelman et al., 1989; Mendelman et al., 1990; Yu et al., 1992; Kati et al., 1992, Johnson, 1993).

The current study provides fidelity estimates for the RNA dependent DNA replication reaction of HIV-1 RT under the same conditions as previously described (Kati et al., 1992). The RNA-dependent fidelity for RT relies solely on the polymerase contribution since there is no exonuclease activity associated with RT and is thus a relationship between the selectivity for correct dNTP discrimination over that of incorrect dNTP. Fidelity may be estimated therefore as a ratio of the k_{pol}/K_d values for correct to incorrect nucleotide

incorporation, as given in Tables 2 and 3. In contrast to previous studies (Kati et al., 1992; Preston et al., 1988; Roberts et al., 1988; Weber et al., 1989; Bebenek et al., 1989; Ji and Loeb, 1992; Perrino et al., 1989; Mendelman et al., 1989; Mendelman et al., 1990; Yu et al., 1992), our results from the present work show HIV-1 RT to be more discriminating to RNA dependent polymerization than previously observed for either DNA or RNA dependent polymerization. A forward mutation assay has suggested a higher fidelity for RNA versus DNA templates for frameshifts (Boyer al., 1992) but not for substitutions. In using an RNA/DNA 45/25 template−primer, the fidelity estimate for misincorporation of a dGMP was 26 000 while those for dCMP and dTMP were 176 000 and approximately 1×10^6, respectively, over a template uridine. These estimates indicate an increased fidelity of HIV-1 RT of 9−64-fold (approximately 1 to 2 orders of magnitude) over that of the corresponding DNA-directed polymerization fidelity of RT, on direct comparison with the previous results (Kati et al., 1992).

The apparent dissociation rate constants (K_d) for the incorrect nucleotide incorporation for RNA-dependent polymerization were similar to those determined previously for the DNA dependent polymerization of RT (Kati et al., 1992). The 50−80-fold difference in binding affinities (Table 2) suggests that incorrect nucleotides do not act as competitive inhibitors of correct nucleotide incorporation. However, the polymerization rates (k_{pol}) differed significantly. In contrast to what was observed with correct dNTP incorporation, RNA dependent polymerization being 2-fold faster than DNA dependent polymerization (Kati et al., 1992), the rates for incorrect nucleotide incorporation with the RNA template were surprisingly slow. Since the DNA dependent polymerization rates for misincorporation were only 7−90-fold slower (for dGMP to dCMP or dTMP) than the corresponding rate for correct incorporation (dAMP) (Kati et al., 1992), a decrease of similar magnitude (7−90-fold) was expected for the RNA dependent misincorporation rates. In contrast to the expectation, the RNA dependent misincorporation rates ranged from 364-fold slower for dGMP to more than 2000-fold slower for dCMP and greater than 21000-fold slower for a dTMP misincorporation, compared to the rate of correct (dAMP) incorporation (Table 2), indicating a highly discriminating enzyme for RNA dependent polymerization. While the misincorporation rate for dGTP (0.203 s^{-1}) was only slightly faster than the product dissociation rate (0.13 s^{-1}), the rates for misincorporation of dCTP (0.033 s^{-1}) and dTTP (0.003 s^{-1}) were 1−2 orders of magnitude slower than the dissociation rate of the enzyme−RNA/DNA complex. Since these experiments were carried under single turnover conditions in which the substrate is stoichiometric with enzyme, the maximum rate of polymerization (k_{pol}) is limited by either a conformational change or chemical catalysis but not product dissociation for the dCTP and dTTP incorporation and is most likely equal to k_{cat} under steady-state conditions. To establish if the higher discrimination with RNA may be a more general property of HIV-1 RT, this analysis was extended to a 45/22 template−primer. In this case the correct and incorrect incorporation opposite a template adenine was examined with both a DNA and an RNA substrate. A 14−23-fold higher fidelity was observed for the RNA template in comparision with the DNA indicating this may be a common feature for HIV-1 RT.

This high degree of selectivity by RT *in vitro* has not been detected prior to our study although more recent results from an *in vivo* study of HIV fidelity (Mansky and Temin, 1995) is consistent with our observations. Previous studies using steady-state analysis (Yu and Goodman, 1992; Ji and Loeb, 1992; Johnson, 1993) have provided RNA dependent fidelity similar to that observed for the DNA replication fidelity estimates. In present investigation to examine RNA dependent fidelity, a pre-steady-state kinetic analysis was undertaken to directly observe the events at the active site of RT. The relative ease with which some mismatches occur with an RNA/DNA template−primer is consistent with earlier studies examining DNA/DNA template−primers (Kati et al., 1992; Ji and Loeb, 1992). For instance, the G/U mismatch was still observed to be the easiest mismatch to form. According the the rates presented in Table 2, the G/U mismatch formed approximately 6-fold faster than C/U and about 60-fold faster than T/U, suggesting that conformational and other thermodynamic factors (Abbots et al., 1991) contribute to the inability of the enzyme to sufficiently discriminate between a dA/T (dA/U) or dG/T (dG/U) base pair. The difference in K_ms for correct versus incorrect dNTP insertion were found to be in general agreement to the differences in K_ds seen in this investigation, as was the ability of RT to extend a mismatch (Figure 3), and continue polymerization (Yu and Goodman, 1992) albeit at a slower rate.

The high fidelity exhibited by HIV-1 RT for the RNA dependent DNA polymerization, as shown in this study, may be anticipated as an essential element for survival of an RNA virus. Since the virus inherently lacks a proofreading mechanism in its replication, the virus must strive to make an efficient and correct first (minus) strand DNA copy. This must be done prior to the degradation of its RNA template. While errors in the second DNA strand synthesis may involve error correction mechanisms, by proofreading using host polymerases (Glazer et al., 1987; Stephenson and Karran, 1989), the first DNA strand synthesis has no such correction mechanism. Thus, in the absence of error-free replication for the RNA dependent polymerization, the final proviral DNA may have imperfections which could have further deleterious consequences for the virus such as production of a nonviable virus. The high fidelity seen in this investigation may perhaps be a necessary mechanism for formation of viable viral particles. The differences in the fidelity estimates seen here and by earlier studies may be due to several factors. By examining the replication fidelity using pre-steady-state kinetic analysis under single turnover conditions, our primary focus was on mechanism by looking directly at the events at the active site of RT. Other studies showing lower RNA dependent fidelity estimates than those reported here have been conducted using steady-state assays (Yu and Goodman, 1992; Johnson, 1993; Johnson, 1992), which may not entirely reflect events at the active site of the enzyme by masking mechanistic detail. The genomic hypervariation that has been observed with HIV-1 viral isolates (Coffin, 1986; Goodenow et al., 1989) has been attributed to decreased fidelity of the RNA dependent DNA replication and may in part be due to other factors such as viral survival. In light of the high fidelity exhibited by RT in this investigation and previous fidelity estimates suggesting RT to be no less efficient than other polymerases (Preston et al., 1988; Mendelman et al., 1989; Takeuchi et al., 1988),

one may speculate that the high degree of genomic variation of HIV-1 may be due more to a defense mechanism of the virus to escape the surveillance of the host immune system than to the "sloppiness" on the part of RT.

The extremely slow reaction rates seen for the RNA dependent mismatch experiments is consistent with the model of a two-step binding mechanism of HIV-1 RT involving a rate-limiting conformational change as previously proposed (Kati et al., 1992; Hsieh et al., 1993; Spence et al., 1995; Rittinger et al., 1995) and similar to the kinetic model seen with T7 DNA polymerase (Patel et al., 1991; Wong et al., 1991; Spence et al., 1995). This model argues that RT or T7 DNA polymerase provides the high fidelity of dNTP incorporation in a two-step mechanism (Spence et al., 1995). In the first step, ground state binding between enzyme in an "open" binding state with template−primer and dNTP is formed, while the second step involves a conformational change to a "closed" state whereby the protein can encompass the template−primer and dNTP so as to form an extremely tight binding template−primer−dNTP complex from which catalysis can occur. It is in this step that fidelity of the protein is most apparent. Catalysis can only occur if the protein can adopt the critical catalytic configuration which is dependent on correct Watson−Crick base pairing with the incoming nucleotide and template (Johnson, 1993). However, if the protein cannot adopt this critical configuration, then the reaction proceeds extremely slowly and this step, perhaps, may be the rate-limiting step in the overall pathway. This extremely slow rate for RNA misincorporation is precisely what is observed in the present investigation. Thus, the high fidelity estimates for the RNA dependent replication reaction are primarily due to the extremely slow reaction rates for incorporation of incorrect dNTPs and is most likely the result of either a conformational change or chemical catalysis being the rate-limiting step.

An intriguing question concerns the mechanistic basis for the discrimination of RNA versus DNA mismatches by HIV RT? The answer, in part, may lie in differences in thermodynamic stability of RNA/DNA heteroduplexes and DNA/DNA duplexes (Fedoroff et al., 1993; Wang et al., 1992; Zhu et al, 1995; Sugimoto, et al., 1995) although our data indicate that efficiency of nucleotide incorporation plays a significant role. Insight into this question would be provided by structural information on HIV RT comparing ternary complexes with an RNA/DNA substrate or DNA/DNA substrate and dNTP bound in the active site; however, these structures are not available at present.

REFERENCES

Abbotts, J., Jaju, M., & Wilson, S. (1991) *J. Biol. Chem. 266*, 3937−3943.

Bebenek, K., Abbotts, J., Roberts, J. D., Wilson, S. H., & Kunkel, T. A. (1989) *J. Biol. Chem. 264*, 16948−16956.

Bebenek, K., Abbotts, J., Wilson, S. H., & Kunkel, T. A. (1993) *J. Biol. Chem. 268*, 10324−10334

Boyer, J. C., Bebenek, K., & Kunkel, T. A. (1992) *Proc. Natl. Acad. Sci. U.S.A. 89*, 6919−6923

Coffin, J. M. (1986) *Cell 46*, 1−4.

Fedoroff, O. Y., Salazar, M., & Reid, B. R. (1993) *J. Mol. Biol. 233*, 509−523.

Glazer, P. M., Sarkar, A. N., Chisholm, G. E., & Summers, W. C. (1987) *Mol. Cell. Biol. 7*, 218−224.

Gopalakrishnan, V., Peliska, J., & Benkovic, S. (1992) *Proc. Natl. Acad. Sci. U.S.A., 89*, 10763−10767

Goodenow, M., Huet, T., Saurin, W., Kwok, S., Sninsky, J., & Wain-Hobson, S. (1989) *J. Acquired Immune Defic. Syndr. 2*, 344−352

Hsieh, J.-C., Zinnen, S., & Modrich, P. (1993) *J. Biol. Chem. 268*, 24607−24613.

Jacobo-Molina, A., Ding, J., Nanni, R. G., Clark, A. D., Jr., Lu, X., Tantillo, C., Williams, R. L., Kamer, G., Ferris, A. L., Clark, P., Hizi, A., Hughes, S. H., & Arnold, E. (1993) *Proc. Natl. Acad. Sci. U.S.A. 90*, 6320−6324.

Ji, J., & Loeb, L. A. (1992) *Biochemistry 31*, 954−958.

Ji, J., & Loeb, L. A. (1994) *Virology 199*, 323−330.

Johnson, K. A. (1986) *Methods Enzymol. 134*, 677−705.

Johnson, K. A. (1992) *The Enzymes 20*, 1−61.

Johnson, K. A. (1993) *Annu. Rev. Biochem. 62*, 685−713.

Kati, W. M., Johnson, K. A., Jerva, L. F., & Anderson, K. S. (1992) *J. Biol. Chem. 267*, 25988−25997.

Kohlstaedt, L. A., Wang, J., Friedman, J., Rice, P. A., & Steitz, T. A. (1992) *Science 256*, 1783−1790.

Kuchta, R. D., Mizrahi, V., Benkovic, P. A., Johnson, K. A., & Benkovic, S. J. (1987) *Biochemistry 26*, 8410−8417.

Kuchta, R. D., Benkovic, P., & Benkovic, S. J. (1988) *Biochemistry 27*, 6716−6725.

Mansky, L. M., & Temin, H. M. (1995) *J. Virol. 69*, 5087−5094.

Mendelman, L. V., Boosalis, M. S., Petruska, J., & Goodman, M. F. (1989) *J. Biol. Chem. 264*, 14415−14423.

Mendelman, L. V., Petruska, J., & Goodman, M. F. (1990) *J. Biol. Chem. 265*, 2338−2346.

Müller, B., Restle, T., Weiss, S., Gautel, M., Sczakiel, G., & Goody, R. S. (1989) *J. Biol. Chem. 264*, 13975−13978.

Patel, S. S., Wong, I., & Johnson, K. A. (1991) *Biochemistry 30*, 511−525.

Perrino, F., Preston, B. D., Sandell, L. L., & Loeb, L. A. (1989) *Proc. Natl. Acad. Sci. U.S.A. 86*, 8343−8347

Preston, B. D., Poiesz, B. J., & Loeb, L. A. (1988) *Science 242*, 1168−1171.

Preston, B. D., Keulen, W., Nijhuis, M., Schuurman, R., Berkhout, B., Boucher, C., Balzarini, J., Pelemans, H., De Clercq, E., Karlsson, A., Kleim, J.-P., Prasad, V. R., Drosopoulos, W. C., Wainberg, M. A. (1997) *Science 275*, 228−231.

Reardon, J. E. (1992) *Biochemistry 31*, 4473−4479.

Reardon, J. E. (1993) *J. Biol. Chem. 268*, 8743−8751.

Ricchetti, M., & Buc, H. (1990) *The EMBO J. 9*, 1583−1593.

Rittinger, K., Divita, G., & Goody, R. S. (1995) *Proc. Natl. Acad. Sci. U.S.A. 92*, 8046−8049.

Roberts, J. D., Bebenek, K., & Kunkel, T. A. (1988) *Science 242*, 1171−1173

Spence, R. A., Kati, W. M., Anderson, K. S., & Johnson, K. A. (1995) *Science 267*, 988−993.

Stahlhut, M., Li, Y., Condra, J. H., Fu, J., Gotlib, L., Graham, D. J., & Olsen, D. (1994) *Protein Expression Purif. 6*, 614−621.

Stephenson, C., & Karran, P. (1989) *J. Biol. Chem. 264*, 21177−21182.

Sugimoto, N., Nakano, S., Katoh, M., Matsumura, A., Nakamuta, H., Ohmichi, T., Yoneyama, M., & Saski, M. (1995) *Biochemistry 34*, 11211−11216.

Takeuchi, Y., Nagumo, T., & Hoshing, H. (1988) *J. Virol. 62*, 3900−3902.

Wang, A. C., Kim, S., Flynn, P., Chou, S.-H., Orban, J., & Reid, B. R. (1992) *Biochemistry 31*, 3940−3946.

Weber, J., & Grosse, F. (1989) *Nucleic. Acids Res. 17*, 1379−1393.

Wong, I., Patel, S. S., & Johnson, K. A. (1991) *Biochemistry 30*, 526−537.

Yu, H., & Goodman, M. F. (1992) *J. Biol. Chem. 267*, 10888−10896.

Zhu, L., Salazar, M., & Reid, R. R. (1995) *Biochemistry 34*, 2372−2380.

Zinnen, S., Hsieh, J. C., & Modrich, P. (1994) *J. Biol. Chem. 269*, 24195−24202.

BI971385+